Evaluation of [^{11}C]S14506 and [^{18}F]S14506 in Rat and Monkey as Agonist PET Radioligands for Brain 5-HT$_{1A}$ Receptors

Shuiyu Lu*, Jeih-San Liow, Sami S. Zoghbi, Jinsoo Hong, Robert B. Innis and Victor W. Pike

Molecular Imaging Branch, National Institute of Mental Health, National Institutes of Health, 10 Center Drive, Room B3C346, Bethesda MD 20892-1003, USA

Abstract: *In vitro* and *ex vivo* measurements have shown that the binding of the selective high-affinity agonist, S14506 (1-[2-(4-fluorobenzoylamino)ethyl]-4-(7-methoxy-naphthyl)piperazine), to 5-HT$_{1A}$ receptors, is similar in affinity (K_d = 0.79 nM) and extent (B_{max}) to that of the antagonist, WAY 100635. We aimed to test whether S14506, labeled with a positron-emitter, might serve as a radioligand for imaging brain 5-HT$_{1A}$ receptors *in vivo* with positron emission tomography (PET). Here we evaluated [^{11}C]S14506 and [^{18}F]S14506 in rat and rhesus monkey *in vivo*. After intravenous administration of [^{11}C]S14506 into rat, radioactivity entered brain, reaching 210% SUV at 2 min. Radioactivity uptake into brain was higher (~ 350% SUV) in rats pre-treated with the P-glycoprotein (P-gp) inhibitor, cyclosporin A. In rhesus monkey, peak brain uptake of radioactivity after administration of [^{11}C]S14506 or [^{18}F]S14506 was also moderate and for [^{11}C]S14506 increased from ~ 170% SUV after 7 min, to 240% SUV in a monkey pre-treated with the P-gp inhibitor, tariquidar. The ratios of radioactivity in 5-HT$_{1A}$ receptor-rich regions, such as cingulate or hippocampus to that in receptor-poor cerebellum reached between 1.35 and 1.5 at 60 min for both [^{11}C]S14506 and [^{18}F]S14506. [^{11}C]S14506 gave one major polar radiometabolite in monkey plasma, and [^{18}F]S14506 gave three and two more polar radiometabolites in rat and monkey plasma, respectively. The rat radiometabolites of [^{18}F]S14506 did not accumulate in brain. [^{18}F]S14506 was not radiodefluorinated in monkey. Thus, despite high-affinity and lack of troublesome brain radiometabolites, both [^{11}C]S14506 and [^{18}F]S14506 were ineffective for imaging rat or monkey brain 5-HT$_{1A}$ receptors *in vivo*, even under P-gp inhibited conditions. Explanations for the failure of these radioligands are offered.

Key Words: 5-HT$_{1A}$ receptors, [^{11}C]S14506, [^{18}F]S14506, Agonist, P-gp substrate, PET imaging.

INTRODUCTION

Brain serotonin 5-HT$_{1A}$ receptors have been implicated in a wide range of neuropsychiatric conditions, including depression [1], anxiety [2], schizophrenia [3] and suicide [4]. Consequently, over the last two decades, there has been great interest to study these receptors in patient populations with molecular imaging and especially with positron emission tomography (PET) [5-7]. Brain 5-HT$_{1A}$ receptors have been successfully imaged with PET in human subjects with a range of antagonist radioligands. The most effective and popular radioligands include [*carbonyl*-^{11}C]WAY-100635 [8], [*carbonyl*-^{11}C]DWAY [9], [^{18}F]MPPF [10,11] and [^{18}F]FCWAY [12] (Chart **1**). These antagonist radioligands measure the sum of G-protein-coupled and non G-protein-coupled 5-HT$_{1A}$ receptors. Some studies have indicated that the receptor-specific binding of such antagonist radioligands has only low sensitivity to endogenous serotonin levels [13-17]. This poses a limitation on the use of these radioligands for more deeply probing the role of serotonin, and its interaction with 5-HT$_{1A}$ receptors, in neuropsychiatric disorders.

Many potent and selective 5-HT$_{1A}$ receptor agonists have been labeled with tritium and used successfully for studying brain 5-HT$_{1A}$ receptors *in vitro* [18,19]. The development of agonist radioligands for PET imaging of brain 5-HT$_{1A}$ receptors *in vivo* had until recently met with only limited success [6]. This had probably been due in part to two major obstacles unique to agonist-type ligands. First, agonists generally bind only to receptors that are coupled to G-protein, which represent only an unknown fraction of the receptors available for binding to an antagonist. Second, the binding of an agonist is expected to be transient, since agonist binding converts the receptor into a G-protein dissociated conformational state that usually has low agonist affinity [20-22]. Nonetheless, at least one promising agonist radioligand, [^{11}C]CUMI-101 (Chart **1**), has been reported recently for imaging brain 5-HT$_{1A}$ receptors [23,24]. Such a radioligand is thought to bind only to the G-protein-coupled receptors and may therefore show greater sensitivity of receptor binding to endogenous 5-HT levels.

S14506 (1-[2-(4-fluorobenzoylamino)ethyl]-4-(7-methoxy-naphthyl)piperazine) (Chart **1**) is one of the most potent and selective agonists known for 5-HT$_{1A}$ receptors [25-27]. Its high sub-nanomolar affinity for rodent and human 5-HT$_{1A}$ receptors is at least 100-fold greater than for adrenergic, dopaminergic, histaminergic, opioidergic, GABAergic, cholinergic and other 5-HT receptors. Under *in vitro* conditions, the receptor binding of [^{3}H]S14506 is 'atypical' for an agonist in that it binds to both the G-protein coupled and uncoupled forms of 5-HT$_{1A}$ receptor with almost equally high affinity [26,28]. This contrasts with the prototypical 5-HT$_{1A}$

*Address correspondence to this author at the Molecular Imaging Branch, National Institute of Mental Health, National Institutes of Health, Building 10, Room B3C346, 10 Center Drive, Bethesda, MD 20892-1003, USA; Fax: + 1 301 480 5112; E-mail: Shuiyu.Lu@mail.nih.gov

1874-4710/10 $55.00+.00

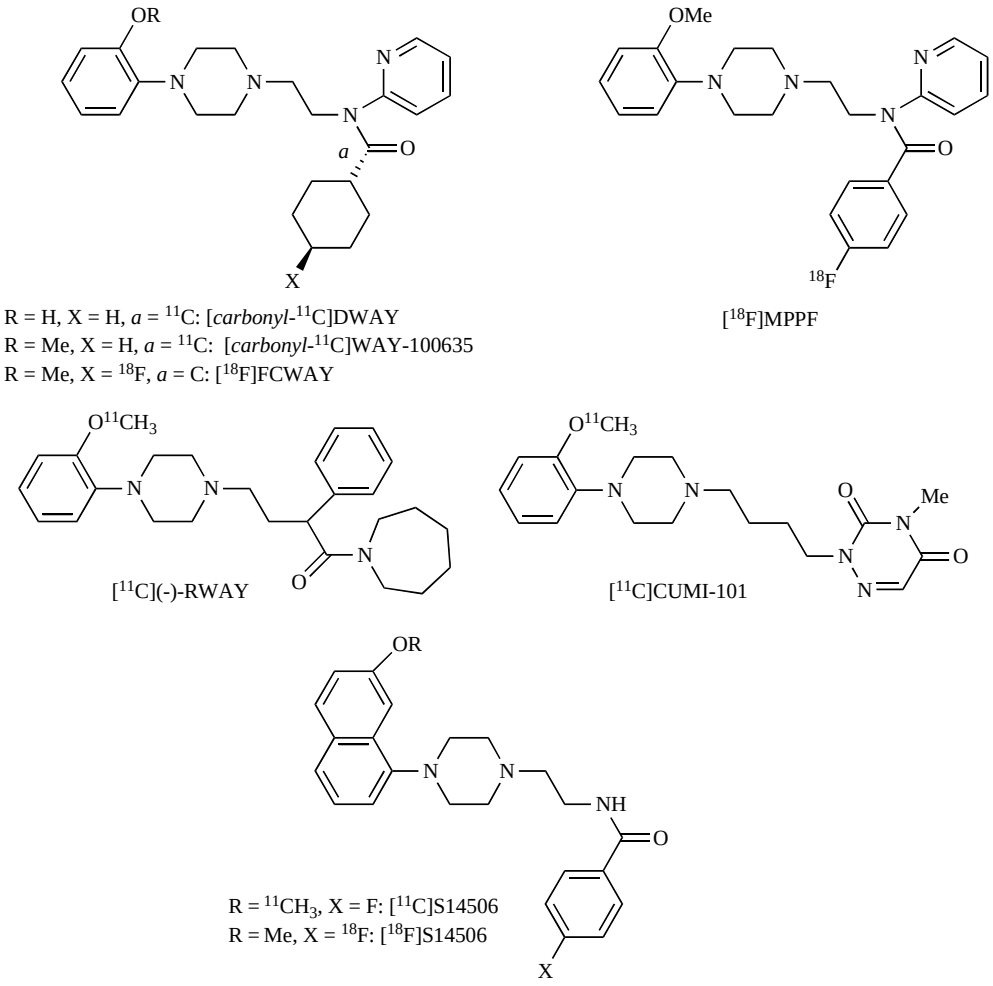

Chart 1. Structures of 5-HT_{1A} receptor antagonists and agonists.

agonist ligand, 8-OH-DPAT, which has a nanomolar affinity for the G-protein coupled form of the receptor only [28].

Lima *et al*. [26] found that at one hour after *i.v.* injection of [^{3}H]S14506 into mice, radioactivity in 5-HT_{1A} receptor-rich hippocampus was 2.5 fold higher than in receptor-poor cerebellum when measured *ex vivo*. They therefore suggested that S14506 could be developed into a PET radioligand for imaging 5-HT_{1A} receptors *in vivo*. We have previously labeled S14506 with either carbon-11 or fluorine-18 [29]. Here we aimed to test [^{11}C]S14506 and [^{18}F]S14506 as radioligands for imaging 5-HT_{1A} receptors *in vivo* with PET. We found that these radioligands provided only very low ratios of receptor-specific to non-specific binding in rat and monkey *in vivo*, and also that they appear to be substrates for the efflux transporter P-gp at the blood-brain barrier in both species.

EXPERIMENTAL

Animal Procedures

All animal procedures were performed in strict accordance with the National Institutes of Health *Guide for Care and Use of Laboratory Animals* [30] and were approved by the National Institute of Mental Health (NIMH) Animal Care and Use Committee.

Materials

No-carrier-added [^{11}C]S14506 and [^{18}F]S14506 were synthesized in high radiochemical purity (> 97%) and formulated for intravenous administration as previously described [29]. For intravenous injection, cyclosporin A (98.5%, Fluka) was formulated in a 1: 3 (v/v) mixture of ethanol and Cremophore EL (BASF) to a final concentration of 75 mg/mL, and diluted twofold with 'Saline for injection'. Tariquidar (XR9576; 7.5 mg/mL for injection; Xenova) was diluted with '5% Dextrose injection' (Baxter) before *i.v.* injection into monkey. Reference S14506, WAY-100635 and DWAY were obtained from Dr. Eric Vermeulen (Groningen University, The Netherlands). Other materials and solvents were purchased from commercial sources and used as received.

General Methods

Moderately high levels of radioactivity (> 0.5 mCi) were measured in a calibrated ionization chamber. Low levels of radioactivity were measured in an automatic well-type γ-counter. All radioactivity measurements were corrected for background and also decay-corrected. Time-activity curves

measured with PET were also decay-corrected. Buffer or biological samples were analyzed for radioligands and their radiometabolites with HPLC on a NovaPak C_{18} column (4 μm; 100 × 8.0 mm i.d.; Waters Corp.), housed within a radial compression module (RCM-100), and eluted at 1.5 or 2.0 mL/min with MeOH: H_2O: Et_3N (80: 20: 0.1 by vol.) [31]. Eluate was monitored for radioactivity and absorbance at 220 nm (Method A). The radiochromatograms were stored and analyzed with "BiochromLite" software (Bioscan) with decay correction of all events to the time of injection onto HPLC. Full recovery of radioactivity from the HPLC column was checked by injection of methanol (2 mL) at the end of each run.

Radioactivity concentrations in biological tissues measured *ex vivo* or with PET *in vivo* were decay-corrected to the time of radioligand administration and expressed as percent standardized uptake value (%SUV), defined as:

$$\frac{Injected\ \ dose\ \ \ per\ \ g\ \ tissue}{Injected\ \ radioactivity} \times g\ \ Body\ \ weight\ \times 100$$

PET Imaging of [^{11}C]S14506 in Rat

For PET imaging experiments, Sprague-Dawley rats (251–549 g) were anesthetized with 1.5% isoflurane. For each experiment, [^{11}C]S14506 was injected as a bolus into each rat *via* the penile vein. Rats were then scanned dynamically for 90 min with the NIH small animal PET Camera (ATLAS) [32,33].

For a P-gp inhibition experiment, one rat (411 g) was scanned at baseline with [^{11}C]S14506 (0.687 mCi) and then treated with cyclosporin A (25 mg/kg, *i.v.)* in Cremophor EL formulation, at 2.5 h after the radioligand injection. After another 30 min, the rat was given a second injection of [^{11}C]S14506 (1.05 mCi) and scanned again. The experiment was repeated in a second rat (325 g) with cyclosporin A administered at a dose of (50 mg/kg, *i.v.*). The first and second doses of [^{11}C]S14506 were 0.825 and 1.30 mCi, respectively. In control experiments, three Sprague-Dawley rats (391–549 g) were also scanned with [^{11}C]S14506 (1.09–1.84 mCi) for 90 min before and after treatment with the cyclosporin A formulation vehicle. Radioligand injections were again 3 h apart.

For a radiotracer displacement experiment, one rat (251 g) was treated with cyclosporin A (25 mg/kg, *i.v.*). Thirty minutes later, the rat was injected with [^{11}C]S14506 (0.818 mCi) followed 13 and 15 min later with DWAY (1 mg/mL; 0.5 mL). The experiment was repeated in a rat of similar weight (259 g) with DWAY (2 mg/kg, *i.v.*; 1.0 mL) administered between 28 and 39 min after radioligand (1.05 mCi).

PET Imaging of [^{18}F]S14506 in Rat

PET imaging was performed in one rat (355 g) as described for imaging with [^{11}C]S14506, except that [^{18}F]S14506 (0.598 mCi; 1.14 Ci/μmol) was used as radioligand. A second rat of similar weight (376 g) was treated with cyclosporin A (50 mg/kg, *i.v.*) in Cremophor EL formulation at 30 min before injection with [^{18}F]S14506 (0.360 mCi; 0.399 Ci/μmol) and PET scanning.

PET Imaging of [^{11}C]S14506 in Monkey

A rhesus monkey (~ 15 kg) was anesthetized with 1.5% isoflurane and injected intravenously with a bolus of [^{11}C]S14506 (3.8 mCi; > 2.0 Ci/μmol) alone and at 3 h later with a second bolus of [^{11}C]S14506 (3.9 mCi; > 1.0 Ci/μmol). WAY 100635 (0.3 mg/kg, *i.v*) was administered at 40 min after the second radioligand injection. Emission data from the brain were acquired for 90 min on an Advance PET camera (GE Healthcare, Waukesha, WI) after each radioligand injection. In a P-gp inhibition experiment on a separate occasion, the same monkey (14.95 kg) was injected with [^{11}C]S14506 (4.06 mCi; 0.722 Ci/μmol) to obtain baseline PET data. At 3 h later the same monkey was injected with tariquidar (4 mg/kg, *i.v.*) and, after another 30 min, again injected with [^{11}C]S14506 (3.7 mCi; 0.833 Ci/μmol). In this experiment, emission data were acquired for 90 min on a High Resolution Research Tomograph (HRRT, Siemens Medical Solutions, Knoxville, TN). Scans were corrected for attenuation and scatter. PET images were co-registered to MRI scans of the same monkey. Cerebellum, hippocampus, frontal cortex and occipital cortex were selected as regions of interest.

PET Imaging of [^{18}F]S14506 in Monkey

Imaging was performed in the HRRT camera under baseline conditions for 120 min in one monkey (11.5 kg), as for the PET imaging of [^{11}C]S14506, except that [^{18}F]S14506 (2.73 mCi; 1.14 Ci/μmol) was used as radioligand.

Stability in Whole Blood, Blood Distribution, and Plasma Protein Binding of [^{11}C]S14506 and [^{18}F]S14506

Rat blood was collected by cardiac puncture, and monkey blood through arterial sampling, each into heparinized vessels.

Radioligand stability in whole blood was determined by adding [^{11}C]S14506 or [^{18}F]S14506 (~ 50 μCi in 5 μL of formulation medium) to rat or monkey whole blood (1.5 mL) and incubating the mixture at room temperature for 125 min. At the end of incubations, plasma was separated from whole monkey or rat blood by centrifugation (1800 g × 3 min). Radioligand binding to plasma proteins was then measured according to Gandelman *et al.* [34]. An aliquot of each plasma sample (200 μL) was also removed and added to a vial containing acetonitrile (500 μL) and reference S14506 (3 μg). Water (200 μL) was added and the sample mixed well again. The tubes containing the plasma-acetonitrile mixtures were centrifuged at 9400 × g for 2 min. Precipitates and supernatant liquids were measured for radioactivity in a γ-counter. Samples of the protein-free supernatant liquids were then analyzed by HPLC Method A. The composition of radioactivity in plasma and brain, in terms of percentages of unchanged radioligand and radiometabolites, was calculated from the acquired chromatographic data.

For the determination of the distribution of [^{18}F]S14506 between blood components, rat whole blood (0.5 mL) was added to two tubes. [^{18}F]S14506 (0.8 μCi) was then added to each tube and incubated at room temperature for 27 min. The blood was centrifuged at 1800 × g for 3 min. Plasma was separated and all components measured for radioactivity in a γ-counter.

Ex Vivo Determination of the Biodistribution of [^{18}F]S14506 in Rat

One Sprague-Dawley rat (362 g) was injected with [^{18}F]S14506 (627 μCi; 0.874 Ci/μmol) at 20 min after administration of cyclosporin A (50 mg/kg, *i.v.*). Thirty minutes after injection of [^{18}F]S14506, one large blood sample was obtained by cardiac puncture, and the brain excised. The cerebellum and the remainder of the brain were resected and immediately placed in pre-weighed tubes containing acetonitrile (1 mL). The tubes were re-weighed and then measured for radioactivity in a γ-counter. The brain tissues were homogenized along with added S14506 (50 μg). After addition of water (200 μL), the brain tissues were again homogenized, re-measured in the γ-counter and then centrifuged at 9400 × g for 2 min. The supernatant liquids were analyzed by HPLC Method A.

Plasma was separated from blood and deproteinized, as described earlier, and then analyzed by HPLC Method A. The composition of radioactivity in plasma and brain, in terms of percentages of unchanged radioligand and radiometabolites, was calculated from the acquired chromatographic data.

The Effect of Cyclosporin A on Rat Plasma and Brain Levels of [^{18}F]S14506

Two rats were used for this study. One (267 g) served as a control. The other (256 g) was treated with cyclosporin A (50 mg/kg, *i.v.*) at 30 min before injection of [^{18}F]S14506. The control and cyclosporin A treated rats were injected with 599 and 601 μCi of [^{18}F]S14506, respectively. Each rat was sacrificed at 30 min after radioligand injection. Blood, cerebrum and cerebellum were resected from each animal. Protein-free plasma was separated from blood, as described above, and analyzed by HPLC Method A. The concentration of unchanged [^{18}F]S14506 in plasma was quantified. Brain and cerebellar radioactivities were measured with a γ-counter.

Measurement of the Emergence of Radiometabolites in Monkey Plasma after [^{11}C]S14506 or [^{18}F]S14506 Administration

Blood was sampled from the femoral artery into heparinized tubes on at least nine known times after administration of either [^{11}C]S14506 or [^{18}F]S14506 to an anaesthetized rhesus monkey ready to be scanned with PET. Sampling times covered the full span of the PET study. Protein-free plasma was separated from blood as described above and then analyzed by HPLC Method A. The composition of radioactivity in plasma, in terms of percentages of unchanged radioligand and radiometabolites, was calculated from the acquired data.

Determination the $LogD_{7.4}$ of S14506 and Computation of $cLogD_{7.4}$ and LogP

The $LogD_{7.4}$ of S14506 was determined using [^{18}F]S14506 (> 99.8% radiochemical purity) with a method described previously [35,36], which is based on the distribution of radioligand between *n*-octanol and sodium phosphate buffer (0.15 M; pH 7.4) at room temperature. c$LogD_{7.4}$ and *LogP* for S14506 were calculated from its structure with Pallas 3.0 software (Compudrug, S. San Francisco, CA).

RESULTS

PET Measurement of Brain Uptake of [^{11}C]S14506 in Rats and Effects of Cyclosporin A and DWAY

Brain time-activity-curves, obtained following administration of [^{11}C]S14506 to two rats, each under baseline and cyclosporin A pretreatment conditions, are shown in Fig. (**1**). Cyclosporin A, at a dose of 25 mg/kg, *i.v.*, increased the early peak whole brain radioactivity from ~ 210 to ~ 310% SUV. A higher cyclosporin A dose (50 mg/kg, *i.v.*) in the second rat further increased peak whole brain radioactivity to ~ 350% SUV. In each experiment, radioactivity in brain decreased steadily to a low level over 90 min. In control experiments, the formulation vehicle of the cyclosporin A dose had no appreciable effects on brain radioactivity uptake and washout (data not shown).

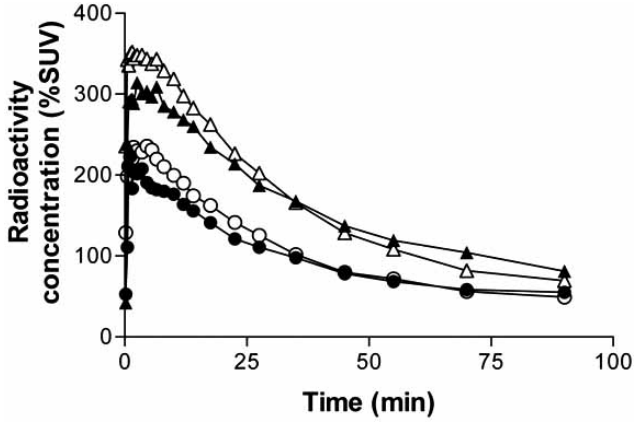

Fig. (1). Whole brain time-activity curves for a single rat administered [^{11}C]S14506 alone (●) or at 30 min after cyclosporin A (25 mg/kg, *i.v.*) (▲), and in another rat administered [^{11}C]S14506 alone (○) or at 30 min after cyclosporin A (50 mg/kg, *i.v.*) (Δ).

In the rat treated with cyclosporin A, preceding [^{11}C]S14506, peak radioactivity uptakes in cerebellum, temporal cortex and frontal cortex were similar, but radioactivity washed out of 5-HT_{1A} receptor poor cerebellum faster than from 5-HT_{1A} receptor-rich cortices (Fig. **2**) and also other regions (not shown). The maximal ratio of radioactivity concentration in temporal cortex to that in cerebellum was about 1.6 at 35 min after injection.

In two experiments, in rats that had been pretreated with cyclosporin A (25 mg/kg, *i.v.*), and administered [^{11}C]S14506 followed by a high dose of DWAY, the rate of radioactivity washout from whole brain noticeably increased after the administration of DWAY (Fig. **3**).

PET Measurement of [^{18}F]S14506 Uptake in Rat Brain and Effect of Cyclosporin A

The peak uptake of radioactivity following injection of [^{18}F]S14506 to rat occurred quickly and was increased by pre-administration of cyclosporin A (Fig. **4**).

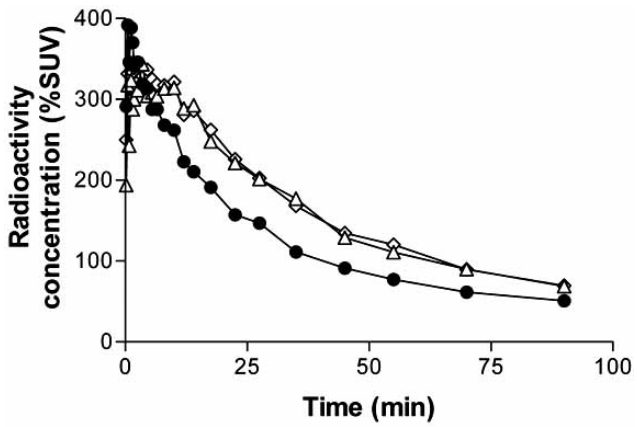

Fig. (2). Time-activity in cerebellum (●), temporal cortex (Δ) and frontal cortex (◊) in a rat pretreated with cyclosporin A (50 mg/kg, *i.v.*) at 30 min before [^{11}C]S14506.

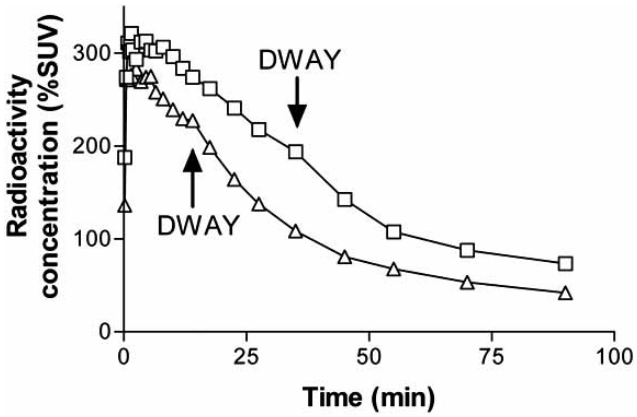

Fig. (3). Whole brain time-activity curves for two rats pre-treated with cyclosporin A (25 mg/kg, *i.v*) and administered [^{11}C]S14506 followed by DWAY (1 mg/kg, *i.v.*) at 13-15 min (Δ) or DWAY (2 mg/kg, *i.v.*) at 28-39 min (□).

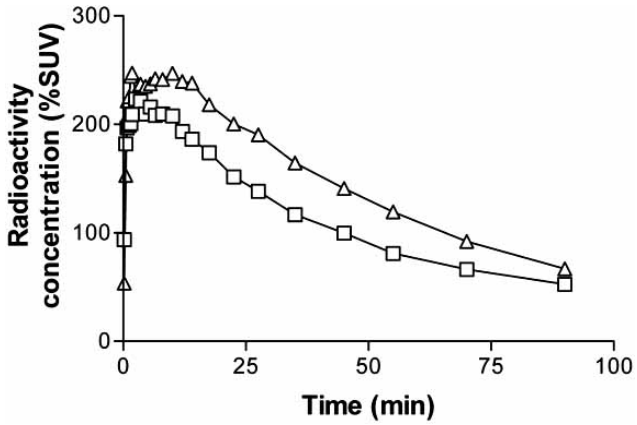

Fig. (4). Whole brain time-activity curves for a rat administered [^{18}F]S14506 alone (□) or in another rat at 30 min after cyclosporin A (50 mg/kg, *i.v.*) (Δ).

PET Measurement of Brain Uptake of [^{11}C]S14506 in Monkey and Effects of WAY-100635 and Tariquidar

After intravenous administration of [^{11}C]S14506 to monkey, radioactivity in whole brain peaked at ~ 170% SUV at 7 min. The initial uptake of radioactivity was similar in all brain regions, but radioactivity washed out slightly slower from 5-HT$_{1A}$ receptor-rich regions, such as cingulate gyrus, temporal cortex and thalamus, than from receptor-poor cerebellum (Fig. **5A**). Ratios of radioactivity in receptor-rich regions to that in cerebellum reached ~ 1.35 at 60 min. In an experiment in which WAY 100635 (0.3 mg/kg, *i.v.*) was given at 40 min after [^{11}C]S14506, radioactivity concentrations in all regions more quickly approached the same terminal level. This appeared to be mainly due to a retarded washout of radioactivity from cerebellum after WAY 100635 administration (Fig. **5B**).

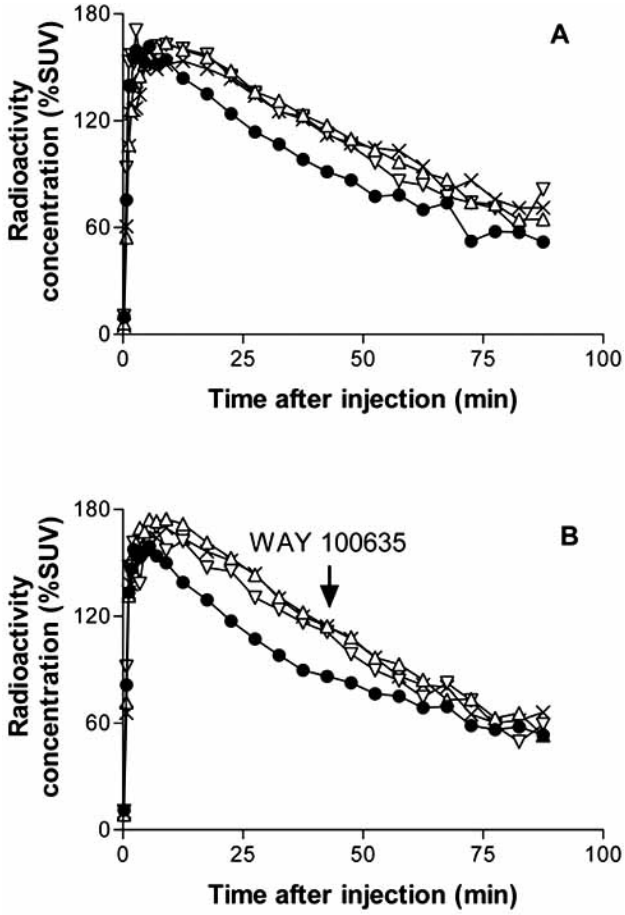

Fig. (5). Uptake of radioactivity (%SUV) into brain regions after intravenous administration of [^{11}C]S14506 to rhesus monkey, under baseline conditions (Panel **A**) and in a displacement experiment (Panel **B**) in which WAY 100635 (0.3 mg/kg, *i.v.*) was given at 40 min after [^{11}C]S14506. Key: ●, cerebellum; Δ, temporal cortex; ▽, thalamus; ×, cingulate.

When the same monkey was treated with tariquidar (4 mg/kg, *i.v.*) at 30 min before administration of [^{11}C]S14506, radioactivity in brain peaked at a higher value (~ 240% SUV; Fig. **6**). The ratios of radioactivity in 5-HT$_{1A}$ receptor-rich regions, such as hippocampus, to that in cerebellum were again about 1.5 at 60 min.

PET Measurement of Brain Uptake of [^{18}F]S14506 in Monkey

After intravenous injection of [^{18}F]S14506 into a rhesus monkey there was moderate uptake of radioactivity into

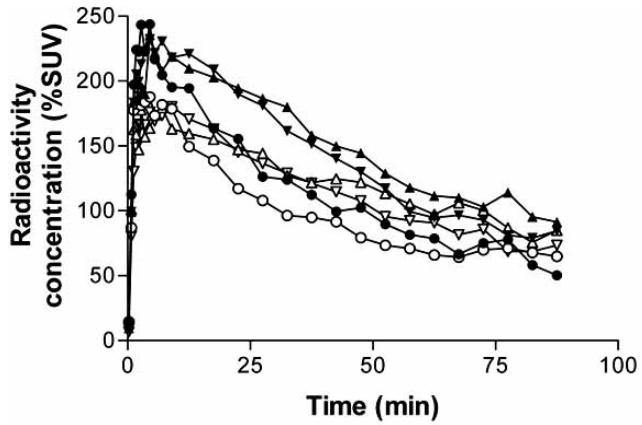

Fig. (6). Time-radioactivity curves in regions of the same rhesus monkey after administration of [^{11}C]S14506 alone (open symbols) or at 30 min after treatment with tariquidar (4 mg/kg, *i.v.*) (solid symbols). Key: o/●, cerebellum; Δ/▲; hippocampus; ▽/▼; occipital cortex.

brain followed by slow washout (Fig. **7**). Radioactivity uptake was initially highest in cerebellum but radioactivity also declined more rapidly in cerebellum than in 5-HT$_{1A}$ receptor-rich regions, such as hippocampus, frontal cortex and occipital cortex.

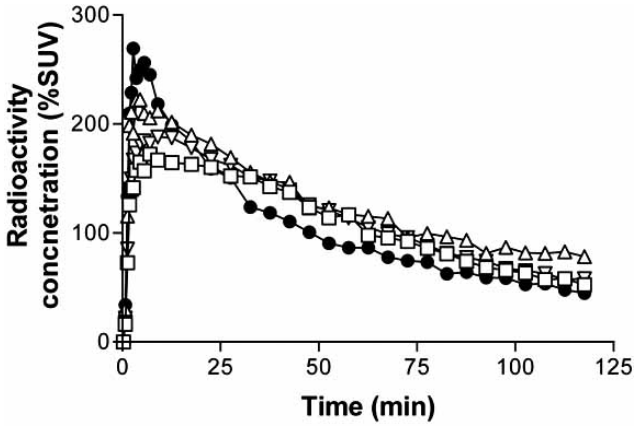

Fig. (7). Time-activity curves in brain regions of monkey after the intravenous injection of [^{18}F]S14506. Key: ●, cerebellum; Δ, hippocampus; □, frontal cortex; ▽, occipital cortex.

Rat Blood Distribution and Protein Binding of S14506

[^{11}C]S14506 was > 99.5% unchanged after incubation with rat whole blood *in vitro* for 125 min. The protein binding of [^{11}C]S14506 and [^{18}F]S14506 in rat plasma was very high, with only 0.52% and 0.61% free in plasma, respectively. The whole blood distribution of [^{11}C]S14506, without hematocrit correction, was 59.1% to plasma and 40.9% to cellular components. The whole blood distribution of [^{18}F]S14506, without hematocrit correction, was 74.2% to plasma and 25.8% to cellular components.

Radiometabolites of [^{18}F]S14506 in Rats

At 30 min after administration of [^{18}F]S14506 to rats, three radiometabolite fractions ([^{18}F]A–C) were detected in plasma (Table **1**). These fractions eluted ahead of [^{18}F]S14506 (t_R = ~ 7.0 min) in the reverse phase HPLC analysis, with retention times of ~ 2.7, 3.8 and 5.5 min for [^{18}F]A, [^{18}F]B and [^{18}F]C, respectively. In brain, the vast majority of the radioactivity was [^{18}F]S14506. Only low amounts of the three radiometabolites appeared in brain. The ratio of brain [^{18}F]S14506 concentration to that in cerebellum was 1.5.

Effect of Cyclosporin A on Rat Plasma and Brain Levels of [^{18}F]S14506

At 30 min after administration of [^{18}F]S14506, control and cyclosporin A treated rats showed similar plasma concentrations of unchanged [^{18}F]S14506 (Table **2**). The ratios of the brain and cerebellum [^{18}F]S14506 concentration to that in plasma were 12.2 and 10.0, in the control rat and 22.9 and 14.0 in the cyclosporin A treated rat, respectively. Thus, cyclosporin A pretreatment increased brain uptake of [^{18}F]S14506 without greatly affecting plasma parent concentration.

Emergence of Radiometabolites of [^{11}C]S14506 in Monkey Plasma

After intravenous administration of [^{11}C]S14506 to monkey, the decrease in radioactivity in plasma was rapid (data not shown). Recoveries of radioactivity from plasma into protein-free plasma for HPLC analysis were uniformly high (94.6 ± 1.9%, n = 20). A single radiometabolite appeared in plasma with a shorter retention time (2.1 ± 0.1 min, n = 22) in the HPLC analysis (eluent flow rate 2.0 mL/min) than [^{11}C]S14506 (t_R = 5.3 ± 0.2 min, n = 22). This much less lipophilic radiometabolite represented half the total radioactivity at 5 min after radioligand injection (Fig. **8**). Another radiometabolite (t_R = 3.5 ± 0.3 min, n = 22) was also observed, but this never became more than 3.1% of the radioactivity in plasma. Pretreatment of the monkey with tariquidar

Table 1. Composition of Radioactivity in Various Rat Tissue Samples at 30 min after Administration of [^{18}F]S14506

Tissue	Composition (%)			
	[^{18}F]S14506	[^{18}F]A	[^{18}F]B	[^{18}F]C
Plasma[a]	38.6 ± 0.17	44.3 ± 9.7	13.8 ± 7.5	2.9 ± 3.0
Cerebellum[b]	93.9	1.5	0.50	3.6
Remainder of brain[c]	97.2 ± 0.20	0.15 ± 0.05	0.45 ± 0.05	2.1 ± 0.1

[a]n = 3 rats (mean ± SD); [b]n = 1 rat; [c]n = 2 rats.

Table 2. Radioactivity Concentrations in Rat Tissues at 30 min after Administration of [^{18}F]S14506 Alone or after Treatment with Cyclosporin A

Tissue	[^{18}F]S14506 Concentration (%SUV)	
	Control	Cyclosporin A treated
Plasma	11.5	9.2
Cerebellum	115	128
Remainder of brain	141	211

did not affect the rate at which radioactivity decreased in plasma (data not shown) nor the emergence of the radiometabolite (Fig. **8**).

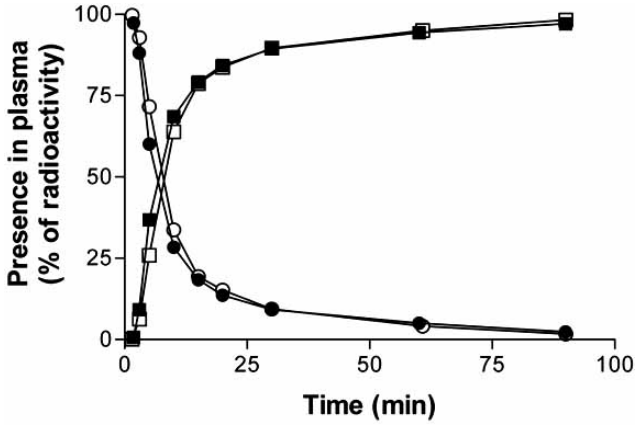

Fig. (8). Composition of radioactivity in plasma after injection of [^{11}C]S14506 into monkey under baseline conditions (closed symbols) and after pre-treatment with tariquidar (4 mg/kg, *i.v.*) (open symbols). Key: o/●, [^{11}C]S14506; □/■, major polar [^{11}C] metabolite.

Emergence of Radiometabolites of [^{18}F]S14506 in Monkey Plasma

Radioactivity concentration reduced rapidly in monkey plasma after the intravenous injection of [^{18}F]S14506 (data not shown). Recoveries of radioactivity from plasma into protein-free plasma for HPLC analysis were uniformly high (95.9 ± 1.7%, n = 31). Two radiometabolite fractions gradually appeared in plasma, [^{18}F]A' and [^{18}F]B', which had shorter retention times of 3.0 ± 0.5 min (n = 34) and 4.9 ± 0.5 min (n = 34) min, respectively, on reverse phase HPLC analysis (eluent flow rate 1.5 mL/min) than parent [^{18}F]S14506 (t_R ~ 8.0 ± 0.1 min, n = 34) (Fig. **9**).

LogD$_{7.4}$, cLogD and LogP of [^{18}F]S14506

[^{18}F]S14506 was stable to incubation in sodium phosphate buffer (0.15 M) at room temperature for 2.5 h. The $LogD_{7.4}$ of [^{18}F]S14506 was found to be 4.14 ± 0.06 (n = 6). The computed value ($cLogD_{7.4}$) was 2.22. The *cLogP* value was calculated to be 3.24.

DISCUSSION

This study demonstrated that S14506, labeled with either carbon-11 or fluorine-18, is ineffective as a radioligand for sensitively imaging brain 5-HT$_{1A}$ receptors in rat or monkey *in vivo* with PET and furthermore indicated that S14506 is a substrate in these two species for the brain efflux transporter, P-gp.

Initial PET imaging experiments in rats showed moderate brain radioactivity uptake after intravenous injection of [^{11}C]S14506 followed by washout of radioactivity down to a very low level at 90 min (Fig. **1**). Several 5-HT$_{1A}$ receptor radioligands of similar structure, based on an aryl-piperazinyl-alkyl backbone, are known to act as substrates for P-gp at the rat blood-brain barrier [37]. These radioligands include [^{18}F]MPPF [38], [^{11}C](–)-RWAY [39] and [^{11}C]WAY 100635 [40] (Chart **1**). In view of the moderate brain uptake of radioactivity, we decided to test the effect of pre-administration of a P-gp inhibitor, cyclosporin A [38-42]. Cyclosporin A has previously been shown to enhance the brain uptake of some P-gp sensitive 5-HT$_{1A}$ receptor radioligands, including [^{18}F]MPPF [38] and [^{11}C](–)-RWAY [39]. This inhibitor also enhanced the uptake of radioactivity into rat brain after administration of [^{11}C]S14506 (Fig. **1**), without increasing the plasma level of radioligand. Further evidence that S14506 is a P-gp substrate in rats was obtained by *ex vivo* measurements at 30 min after administration of [^{18}F]S14506 (Table **2**). We found that, at 30 min after administration of [^{18}F]S14506 to rat, almost all the radioactivity in brain was unchanged radioligand, with very low contamination by any of the three less lipophilic radiometabolites appearing in plasma (Table **1**). Treatment of a rat with

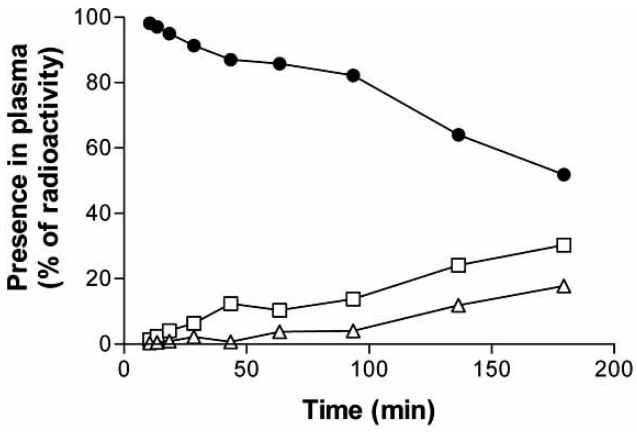

Fig. (9). Time course of the composition of radioactivity in monkey plasma after an injection of [^{18}F]S14506. Key: ●, [^{18}F]S14506; □, [^{18}F]A'; Δ, [^{18}F]B'.

cyclosporin A, preceding administration of [^{18}F]S14506, also increased radioactivity content in brain. Radioactivity concentration in plasma was not increased, implying that the increased brain uptake of radioactivity was due to inhibition of P-gp rather than to an increase in plasma input of radioligand.

In this experiment with *ex vivo* measurements, the ratio of radioactivity in the cerebrum, which contains several extensive 5-HT$_{1A}$ receptor-rich regions, such as cortical regions, cingulate and hippocampus [43], was higher than in receptor-poor cerebellum, indicating a small ratio of receptor-specific binding to non-specific binding of at least 1.65. This ratio, which is for global cerebrum, is somewhat lower, but possibly consistent with the hippocampus to cerebellum radioactivity ratio (2.5 at 60 min) observed *ex vivo* by Lima *et al*. [26] after injection of [^{3}H]S14506 into mice.

In the rat imaging experiment in which brain uptake of radioactivity was highest, namely the experiment in which a high dose of cyclosporin A (50 mg/kg, *i.v.)* was given before [^{11}C]S14506, radioactivity declined faster in cerebellum than in 5-HT$_{1A}$ receptor-rich regions (Fig. **2**). The maximal ratio of radioactivity concentration in temporal cortex to that in cerebellum reached 1.60 at 35 min. This ratio denotes a low level of receptor-specific binding as found in the *ex vivo* rat brain measurements. Imaging of regions in rat brain is subject to partial volume effects because of the small size of the regions in relation to the achievable physical resolution of the PET camera (~ 1.6 mm FWHM). Partial volume effects cause a net 'spill-over' of radioactivity from high radioactivity regions to nearby low radioactivity regions. Hence, PET measurements in small animal brains tend to under-estimate ratios of receptor-specific to non-specific binding. True values may be measured *ex vivo*. By comparing the reported binding of [^{3}H]WAY 100635 to mouse [44] and rat brain regions [43] *in vivo*, it seems reasonable to assume that brain regional 5-HT$_{1A}$ receptor densities are quite similar between these species. The partial volume effect may therefore largely explain why the proportion of receptor-specific binding seen with PET imaging in rat is lower than that determined by previous *ex vivo* measurements in mice [26].

In PET imaging experiments with [^{11}C]S14506 in cyclosporin A pretreated rats, administration of the high-affinity selective 5-HT$_{1A}$ antagonist, DWAY [9], during scans accelerated the washout of radioactivity from whole brain (Fig. **3**). This again indicated a low proportion of specific radioligand binding in brain.

The effects of possible radiometabolites of [^{11}C]S14506 in imaging experiments were unknown. In view of the finding that rat plasma radiometabolites of [^{18}F]S14506 do not readily enter brain (Table **1**), PET imaging was also performed in a rat with [^{18}F]S14506, with and without cyclosporin A pretreatment (Fig. **4**). Again cyclosporin A pretreatment increased peak brain uptake of radioactivity. The time-activity curves for whole brain had a similar shape to those seen in the corresponding experiments with [^{11}C]S14506 (Fig. **1**), thereby suggesting that brain entry of radiometabolites from plasma was not very significant for either radioligand [45].

Clearly, neither [^{11}C]S14506 nor [^{18}F]S14506 is effective for sensitive imaging of rat brain 5-HT$_{1A}$ receptors with PET. We therefore decided to test these radioligands in a larger species closer to human, namely rhesus monkey.

In an experiment in which a monkey was injected with [^{11}C]S14506 alone, the uptake of radioactivity in brain regions peaked quickly at about 170% SUV, and was followed by a continuous decrease to a low level over 90 min (Fig. **5A**). The decrease was faster in receptor-poor cerebellum than in 5-HT$_{1A}$ receptor rich regions, such as cingulate, temporal cortex and thalamus. This suggested the existence of a low proportion of receptor-specific binding in 5-HT$_{1A}$ receptor-rich regions. In a second experiment, the high affinity selective 5-HT$_{1A}$ receptor antagonist, WAY 100635, was administered at 40 min after radioligand. This reduced radioactivity concentrations in all regions to the same low level by 90 min, mainly due to a decrease in the rate of radioactivity washout from cerebellum, rather than to any change in the rate of washout from receptor-rich regions (Fig. **5B**). A possible explanation of this finding is that WAY-100635 caused an increase in radioligand delivery to brain from plasma, possibly as a result of displacement of [^{11}C]S14506 into plasma from peripheral binding sites.

In view of the moderate uptake of radioactivity in brain and the observed sensitivity of [^{11}C]S14506 to rat P-gp, we also tested this radioligand for sensitivity to P-gp in monkey. We chose to use the safer P-gp inhibitor, tariquidar [46-48], since cyclosporin A is severely immunosuppressive and unsuitable for nonhuman primates. In a monkey pre-dosed with tariquidar at 4 mg/kg, peak brain radioactivity increased from ~ 170 to ~ 240% SUV. Thus, S14506 appears to be a substrate for both rat and monkey P-gp. This is unlike the 5-HT$_{1A}$ receptor radioligand [^{11}C](–)-RWAY which shows species differences in P-gp sensitivity [39, 48]. The effect of higher doses of tariquidar on the brain uptake of radioactivity was not tested. The structural features of S14506 responsible for conferring P-gp sensitivity may include the *p*-fluorobenzoyl group as in highly P-gp sensitive MPPF, and/or the aryl-piperazinyl head as in WAY-100635 a more weakly P-gp sensitive ligand (Chart **1**).

In the tariquidar pretreatment experiment, radioactivity decreased more rapidly in cerebellum than from 5-HT$_{1A}$ receptor-rich regions, such as hippocampus and occipital cortex (Fig. **6**). The maximal ratio of radioactivity concentration in hippocampus to that in cerebellum was 1.36 at 57.5 min. PET imaging of a monkey administered [^{18}F]S14506 alone gave similar brain radioactivity uptake and time-activity curves as [^{11}C]S14506 (Fig. **7**).

The decrease in plasma radioactivity after [^{11}C]S14506 administration to monkey was rapid. A much less lipophilic radiometabolite emerged in plasma and represented 50% of radioactivity in plasma at 5 min (Fig. **8**). The identity of this radiometabolite is unknown, but given its polarity it might be a single carbon species arising from *N*-demethylation. Such a plasma radiometabolite would not be expected to accumulate in brain. A second very minor radiometabolite was also observed.

The decrease in plasma radioactivity after [^{18}F]S14506 administration to monkey was also fast. Two less lipophilic

radiometabolites slowly emerged in plasma (Fig. **9**). Their identities are unknown. An absence of radioactivity accumulation in monkey skull suggested that neither was [^{18}F]fluoride ion. One may be a phenol from *N*-demethylation as suspected to occur for [^{11}C]S14506. Another may be [^{18}F] fluorobenzoic acid from amide hydrolysis. Given the similarity in the cerebellar time-activity curves after administration of [^{11}C]S14506 and [^{18}F]S14506, there is probably little accumulation of ^{11}C-labeled or ^{18}F-labeled radiometabolite in monkey brain, as also observed for [^{18}F]S14506 in rat (Table **1**).

As in rat, [^{11}C]S14506 and [^{18}F]S14506 are ineffective radioligands for quantifying brain 5-HT$_{1A}$ receptors in monkey brain *in vivo*. It is unclear whether the very small specific signals derive from binding to G-protein coupled or non-coupled receptors, or both. How may the lack of efficacy of these radioligands be explained? A lack of 5-HT$_{1A}$ receptor affinity is not an explanation, since the affinity is well characterized as sub-nanomolar for rat (K_d = 0.2–0.3 nM) [28] and human (K_d = 0.13 nM) [27] receptors, and is similar to that of successful antagonist radioligands, such as WAY-100635 (K_d = 0.1 nM) [5], and the promising agonist radioligand [^{11}C]CUMI-101 (K_i = 0.15 nM) [23]. A possible factor is that the off rate for S14506 from the receptor is too fast. A finding of an off rate for S14506 from human 5-HT$_{1A}$ receptors in recombinant Chinese hamster ovary cells of 0.029 min^{-1} at room temperature [27], corresponding to a half-life for dissociation of 23.9 min appears consistent with this suggestion, as do the time-activity curves for radioactivity decrease from 5-HT$_{1A}$ receptor-rich regions in this study. A further factor may be that S14506 is just too lipophilic. Computation of *cLogD* for S14506 from structure gave a value of 2.22, which is usually regarded as an acceptable value for candidate PET radioligands [49]. However, measurement of *LogD* gave a value of 4.14 which may be regarded as too high. The very high percentage of radioligand binding to rat plasma proteins reflects this high lipophilicity. Moreover, in monkey, despite the rapid clearance of S14506 from plasma, the decline in non-specific binding in brain, as represented by cerebellar time-activity curves was quite slow. Generally, a 50% decrease in cerebellar radioactivity required > 32 min. Successful 5-HT$_{1A}$ receptor radioligands, including the antagonists [*carbonyl*-^{11}C]WAY 100635 [50, 51] and [*carbonyl*-^{11}C]DWAY [52] and the agonist [^{11}C]CUMI-101 [23,24] show much faster decreases of radioactivity from primate cerebellum. Thus, [^{11}C]S1406 and [^{18}F] S14506 show too fast a decrease in specific binding and too slow a decrease in non-specific binding in living brain.

CONCLUSIONS

[^{11}C]S14506 and [^{18}F]S14506 are ineffective for sensitive measurement of brain 5-HT$_{1A}$ receptors with PET *in vivo*, and are furthermore P-gp substrates. Our findings here will help guide future agonist radioligand development.

ACKNOWLEDGEMENTS

This work was supported by the Intramural Research Program of the National Institutes of Health (National Institute of Mental Health; project #s, Z01-MH-002793 and Z01-MH-002795). We are grateful to Drs. J. A. McCarron and J. L. Musachio for assistance in radioligand production and Mr. R.L. Gladding for assistance in imaging. The authors also thank Xenova for providing XR9576 (tariquidar) and BASF for providing Cremophor EL.

REFERENCES

[1] Arango, V.; Underwood, M.D.; Boldrimi, M.; Tamir, H.; Kassir, S.A.; Hsiung, S.-C.; Chen, J.J.-X.; Mann, J.J. Serotonin 1A receptors, serotonin transporter binding and serotonin transporter mRNA expression in the brainstem of depressed suicide victims. *Neuropsychopharmacology*, **2001**, *25*, 892-903.

[2] Sullivan, G.M.; Oquendo, M.A.; Simpson, N.; Van Heertum, R.L.; Mann, J.J.; Parsey, R.V. Brain serotonin$_{1A}$ receptor binding in major depression is related to psychic and somatic anxiety. *Biol. Psychiatry*, **2005**, *58*, 947-954.

[3] Meltzer, H.Y.; Li, Z.; Kaneda, Y.; Ichikawa, J. Serotonin receptors: their key role in drugs to treat schizophrenia. *Prog. Neuropsychopharm. Biol. Psychiatry*, **2003**, *27*, 1159-1172.

[4] Arango, V.; Huang, Y.Y.; Underwood, M.D.; Mann, J.J. Genetics of the serotonergic system in suicidal behavior. *J. Psychiatr Res*., **2003**, *37*, 375-386.

[5] Fletcher, A.; Pike, V.W.; Cliffe, I.A. Visualization and characterization of 5-HT receptors and transporters *in vivo* and in man. *Sem. Neurosci.*, **1995**, *7*, 421-431.

[6] Pike, V.W.; Halldin, C.; Wikström, H.V. Radioligands for the study of brain 5-HT$_{1A}$ receptors *in vivo*. in Progress in Medicinal Chemistry King, F.D., Oxford, A.W. Eds. Elsevier Science B.V.: Amsterdam, *Prog. Med. Chem*., **2001**, *38*, 189-247.

[7] Passchier, J.; van Waarde, A. Visualisation of serotonin-1A (5-HT$_{1A}$) receptors in the central nervous system. *Eur. J. Nucl. Med*., **2001**, *28*, 113-129.

[8] Pike, V. W.; McCarron, J. A.; Lammertsma, A. A.; Osman, S.; Hume, S. P.; Sargent, P. A.; Bench, C. J.; Cliffe, I. A.; Fletcher, A.; Grasby, P. M. Exquisite delineation of 5-HT$_{1A}$ receptors in human brain with PET and [*carbony*-^{11}C]WAY-100635. *Eur. J. Pharmacol*., **1996**, *301*, R5-R7.

[9] Pike, V.W.; Halldin, C.; McCarron, J.A.; Lundkvist, C.; Hirani, E.; Olsson, H.; Hume, S.P.; Karlsson, P.; Osman, S.; Swahn, C.-G.; Hall, H.; Wikström, H.; Mensonidas, M.; Poole, K.G;. Farde, L. [*Carbonyl*-^{11}C]desmethyl-WAY-100635 (DWAY) is a potent and selective radioligand for central 5-HT$_{1A}$ receptors *in vitro* and *in vivo*. *Eur. J. Nucl. Med.*, **1998**, *25*, 338-346.

[10] Shiue, C.-Y.; Shiue G.G., Mozley, P.D.; Kung, M.-P.; Zhuang, Z.P.; Kim, H.-J.; Kung, H.F. *p*-[^{18}F]-MPPF: A potential radioligand for PET studies of 5-HT$_{1A}$ receptors in humans. *Synapse*, **1997**, *25*, 147-154.

[11] Passchier, J.; van Waarde, A.; Pieterman, R.M.; Elsinga, P.H.; Pruim, J.; Hendrikse, H.N.; Willemsen, A.T.M.; Vaalburg, W. Quantitative imaging of 5-HT$_{1A}$ receptor binding in healthy volunteers with [^{18}F]*p*-MPPF. *Nucl. Med. Biol*., **2000**, *27*, 473-476.

[12] Carson, R.E.; Lang, L.X.; Watabe, H.; Der, M.G.; Adams, H.R.; Jagoda, E.; Herscovitch, P.; Eckelman, W.C. PET evaluation of [^{18}F]FCWAY, an analog of the 5-HT$_{1A}$ receptor antagonist, WAY-100635. *Nucl. Med. Biol*., **2000**, *27*, 493-497.

[13] Hume, S.; Hirani, E.; Opacka-Juffry, J.; Myers, R.; Townshend, C.; Pike, V.; Grasby, P. Effect of 5-HT on binding of [^{11}C]WAY 100635 to 5-HT$_{1A}$ receptors in rat brain, assessed using *in vivo* microdialysis and PET after fenfluramine. *Synapse*, **2001,** *41*, 150-159.

[14] Maeda, J.; Suhara, T.; Ogawa, M.; Okauchi, T.; Kawabe, K.; Zhang, M.R.; Semba, J.; Suzuki, K. *In vivo* binding properties of [*carbonyl*-^{11}C]WAY-100635: Effect of endogenous serotonin. *Synapse*, **2001**, *40*, 122-129.

[15] Udo De Haes, J.I.; Cremers, T.I.F.H.; Bosker, F.J.; Postema, F.; Tiemersma-Wegman, T.D.; den Boer, J.A. Effect of increased serotonin levels on [^{18}F]MPPF binding in rat brain: fenfluramine *vs* the combination of citalopram and ketanserin. *Neuropsychopharmacology*, **2005**, *30*, 1624-1631.

[16] Udo De Haes, J.I. ; Harada, N.; Elsinga, P.H.; Maguire, R.P.; Tsukada, H. Effect of fenfluramine-induced increases in serotonin release on [^{18}F]MPPF binding: a continuous infusion PET study in conscious monkeys. *Synapse*, **2006**, *59*, 18-26.

[17] Jagoda, E.M.; Lang, L.X.; Tokugawa, J.; Simmons, A.; Ma, Y.; Contoreggi, C.; Kiesewetter, D.; Eckelman, W.C. Development of

5-HT_{1A} receptor radioligands to determine receptor density and changes in endogenous 5-HT. *Synapse*, **2006**, *59*, 330-341.

[18] Hamon, M. Serotoninergic neurons and 5-HT receptors in the CNS. handbook of experimental pharmacology, *129*. Baumgarten, H.G.; Göthert, M. Eds. Springer-Verlag: Berlin, **1997**, pp. 239-268.

[19] Lanfumey, L.; Hamon, M. Central 5-HT_{1A} receptors: regional distribution and functional characteristics. *Nucl. Med. Biol.*, **2000**, *27*, 429-435.

[20] Strange, P.G. Agonist binding to G-protein coupled receptors. *Br. J. Pharm.*, **2000**, *129*, 820-821.

[21] McLoughlin, D.J.; Strange, P.G. Mechanisms of agonism and inverse agonism at serotonin 5-HT_{1A} receptors. *J. Neurochem.*, **2000**, *74*, 347-357.

[22] Newman-Tancredi, A.; Verrièle, L.; Millan, M.J. Differential modulation by GTPγS of agonist and inverse agonist binding to h5-HT_{1A} receptors revealed by [^{3}H]-WAY100635. *Br. J. Pharm.*, **2001**, *132*, 518-524.

[23] Kumar, J.S.D.; Prabhakaran, J.; Majo, V.J.; Milak, M.S.; Hsiung, S.C.; Tamir, H.; Simpson, N.R.; Van Heertum, R.L.; Mann, J.J.; Parsey, R.V. Synthesis and *in vivo* evaluation of a novel 5-HT_{1A} receptor agonist radioligand [*O*-methyl-^{11}C]2-(4-(4-(2-methoxyphenyl)piperazin-1-yl)butyl)-4-methyl-1,2,4-triazine-3,5(2*H*,4*H*)dione in nonhuman primates. *Eur. J. Nucl. Med. Mol. Imaging*, **2007**, *34*, 1050-1060.

[24] Milak, M.S.; Severance, A.J.; Ogden, R.T.; Prabhakaran, J.; Kumar, J.S.D.; Majo, V.J.; Mann J.J.; Parsey R.V. Modeling considerations for ^{11}C-CUMI-101, an agonist radiotracer for imaging serotonin 1A receptor *in vivo* with PET. *J. Nucl. Med*., **2008**, *49*, 587-596.

[25] Colpaert, F.C.; Koek, W.; Lehmann, J.; Rivet, J.M.; Lejeune, F.; Canton, H.; Bervoets, K.; Millan, M.J.; Laubie, M.; Lavielle, G. S14506: A novel, potent, high-efficacy 5-HT_{1A} agonist and potential anxiolytic agent. *Drug Dev. Res.*, **1992**, *26*, 21-48.

[26] Lima, L.; Laporte, A. M.; Gaymard, C.; Spedding, M.; Mocaër, E.; Hamon, M. Atypical *in vitro* and *in vivo* binding of [^{3}H]S-14506 to brain 5-HT_{1A} receptors. *J. Neural. Transm.*, **1997**, *104*, 1059-1075.

[27] Milligan, G.; Kellett, E.; Dacquet, C.; Dubreuil, V.; Jacoby, E.; Millan, M.J.; Lavielle, G.; Spedding, M. S14506: novel receptor coupling at 5-HT_{1A} receptors. *Neuropharmacology*, **2001**, *40*, 334-344.

[28] Assié, M.-B.; Cosi, C.; Koek, W. Correlation between low/high affinity ratios for 5-HT_{1A} receptors and intrinsic activity. *Eur. J. Pharmacol.*, **1999**, *386*, 97-103.

[29] Lu, S.Y.; Hong, J.S.; Musachio, J.L.; Chin, F.T.; Vermeulen, E.S.; Wikström, H.V.; Pike, V.W. Alternative methods for labeling the 5-HT_{1A} receptor agonist, 1-[2-(4 fluorobenzoylamino)ethyl]-4-(7-methoxynaphthyl)piperazine (S14506), with carbon-11 or fluorine-18. *J. Label. Compd. Radiopharm*., **2005**, *48*, 971-981.

[30] Clark, J.D.; Baldwin, R.L.; Bayne, K.A.; Brown, M.J.; Gebhart, G.F.; Gonder, J.C.; Gwathmey, J.K.; Keeling, M.E.; Kohn, D.F.; Robb, J.W.; Smith, O.A.; Steggerda, J.A.-D.; VandeBer, J.L. *Guide for the Care and Use of Laboratory Animals*; National Academy Press: Washington DC, **1996**.

[31] Zoghbi, S.S.; Shetty, H.U.; Ichise, M.; Fujita, M.; Imaizumi, M.; Liow, J.S.; Shah, J.; Musachio, J.L.; Pike, V.W.; Innis, R.B. PET imaging of the dopamine transporter with ^{18}F-FECNT: a polar radiometabolite confounds brain radioligand measurements. *J. Nucl. Méd.*, **2006**, *47*, 520-527.

[32] Seidel, J.; Vaquero, J.J.; Green, M.V. Resolution uniformity and sensitivity of the NIH ATLAS small animal PET scanner: comparison to simulated LSO scanners without depth-of-interaction capability. *IEEE Trans. Nucl. Sci.*, **2003**, *50*, 1347-1350.

[33] Toyama, H.; Ye, D.; Ichise, M.; Liow, J.S.; Cai, L.S.; Jacobowitz, D.; Musachio, J.L.; Hong J.; Crescenzo, M.; Tipre, D.; Lu, J.-Q.; Zoghbi, S.; Vines, D.C.; Seidel, J.; Katada, K.; Green, M.V.; Pike, V.W.; Cohen, R.M.; Innis, R.B. PET imaging of brain with the beta-amyloid probe, [^{11}C]6-OH-BTA-1, in a transgenic mouse model of Alzheimer's disease, *Eur. J. Nucl. Med. Mol. Imaging*, **2005**, *32*, 593-600.

[34] Gandelman, M.; Baldwin, R.M.; Zoghbi, S.S.; Zea-Ponce, Y.; Innis, R.B. Evaluation of ultrafiltration for the free fraction determination of SPECT radiotracers: ß-CIT, IBF, and iomazenil. *J. Pharm. Sci.*, **1994**, *83*, 1014-1019.

[35] Zoghbi, S.S.; Baldwin, R.M.; Seibyl, J.S.; Charney, D.S.; Innis R.B. A radiotracer technique for determining apparent pKa of receptor-binding ligands. *J. Label. Compds. Radiopharm.*, **1997**, *40* (Suppl. 1), 136-138.

[36] Briard, E.; Zoghbi S.S.; Imaizumi, M.; Gourley, J.P.; Shetty, H.U.; Hong, J.; Cropley, V.; Fujita, M.; Innis, R.B.; Pike, V.W. Synthesis and evaluation in monkey of two sensitive ^{11}C-labeled aryloxyanilide ligands for imaging brain peripheral benzodiazepine receptors *in vivo*. *J. Med. Chem*., **2008**, *51*, 17-30.

[37] Fromm, M.F. Importance of P-glycoprotein at blood-tissue barriers. *Trends Pharm. Sci.*, **2004**, *25*, 423-429.

[38] Passchier, J.; van Waarde, A.; Doze, P.; Elsinga, P.H.; Vaalburg, W. Influence of P-glycoprotein on brain uptake of [^{18}F]MPPF in rats. *Eur. J. Pharm.*, **2000**, *407*, 273-280.

[39] Liow, J.S.; Lu, S.-Y.; McCarron, J.A.; Hong, J.S.; Musachio, J.L.; Pike, V.W.; Innis, R.B.; Zoghbi, S.S. Effect of a P-glycoprotein inhibitor, Cyclosporin A, on the disposition in rodent brain and blood of the 5-HT_{1A} receptor radioligand, [^{11}C](*R*)-(-)-RWAY. *Synapse*, **2007**, *61*, 96-105.

[40] Elsinga, P.H.; Hendrikse N.H.; Bart, J.; van Waarde, A.; Vaalburg, W. Positron emission tomography studies on binding of central nervous system drugs and P-glycoprotein function in the rodent brain. *Mol. Imaging Biol*., **2005**, *7*, 37-44.

[41] Hughes, C.S.; Vaden, S.L.; Manaugh, C.A.; Price, G.S.; Hudson, L.C. Modulation of doxorubicin concentration by cyclosporin A in brain and testicular barrier tissues expressing P-glycoprotein in rats. *J. Neurol. Oncol.*, **1998**, *37*, 45-54.

[42] Syvänen, S.; Blomquist, G.; Sprycha, M.; Höglund, A.U.; Roman, M.; Eriksson, O.; Hammarlund-Udenaes, M.; Långström, B.; Bergström, M. Duration and degree of cyclosporin induced P-glycoprotein inhibition in the rat blood-brain barrier can be studied with PET. *Neuroimage*, **2006**, *32*, 1134-1141.

[43] Hume, S.P.; Ashworth, S.; Opacka-Juffry, J.; Ahier, R.G.; Lammertsma, A.A.; Pike, V.W.; Cliffe, I.A.; Fletcher, A.; White, A.C. Evaluation of [O-*methyl*-^{3}H]WAY-l00635 as an *in vivo* radioligand for 5-HT_{1A} receptors in rat brain. *Eur. J. Pharmacol*., **1994**, *271*, 515-523.

[44] Laporte, A.-M.; Lima, L.; Gozlan, H.; Hamon, M. Selective *in vivo* labelling of brain 5-HT_{1A} receptors by [^{3}H]WAY 100635 in the mouse. *Eur. J. Pharmacol*., **1994**, *271*, 505-514.

[45] Gatley, S.J.; Yu, D.W.; Fowler, J.S.; MacGregor, R.R.; Schlyer, D.J.; Dewey, S.L.; Wolf, A.P.; Martin, T.; Shea, C.E.; Volkow, N.D. Studies with differentially labeled [^{11}C]cocaine, [^{11}C]norcocaine, [^{11}C]benzoylecgonine, and [^{11}C]- and 4'-[^{18}F]fluorococaine to probe the extent to which [^{11}C]cocaine metabolites contribute to PET images of the baboon brain. *J. Neurochem*., **1994**, *62*, 1154-1162.

[46] Martin, C.; Berridge, G.; Mistry, P.; Higgins, C.; Charlton, P.; Callaghan. R. The molecular interaction of the high affinity reversal agent XR9576 with P-glycoprotein. *Br. J. Pharm*., **1999**, *128*, 403-411.

[47] Bankstahl, J.P.; Kuntner, C.; Abrahim, A.; Karch, R.; Stanek, J.; Wanek, T.; Wadsak, W.; Kletter, K.; Müller, M.; Löscher, W.; Langer, O. Tariquidar-induced P-glycoprotein inhibition at the rat blood-brain barrier studied with (*R*)-^{11}C-verapamil and PET. *J. Nucl. Med*., **2008**, *49*, 1328-1335.

[48] Yasuno, F.; Zoghbi, S.S.; McCarron, J.A.; Hong, J.S.; Ichise, M.; Gladding, R.L.; Brown, A.K.; Bacher, J.D.; Pike, V.W.; Innis R.B. Quantification of serotonin 5-HT_{1A} receptors in monkey brain with [^{11}C](*R*)-(-)-RWAY. *Synapse*, **2006**, *60*, 510-520.

[49] Waterhouse, R.N. Determination of lipophilicity and its use as a predictor of blood-brain barrier penetration of molecular imaging agents. *Mol. Imaging Biol*., **2003**, *5*, 376-389.

[50] Farde, L.; Ito, H.; Swahn, C.-G.; Pike, V. W.; Halldin, C. Quantitative analyses of carbonyl-carbon-11-WAY-100635 binding to central 5-hydroxytryptamine-1A receptors in man. *J. Nucl. Med.*, **1998**, *39*, 1965-1971.

[51] Gunn, R.N.; Sargent, P.A.; Bench, C.J .; Rabiner E.A.; Osman S.; Pike V.W.; Hume S.P.; Grasby, P.M.; Lammertsma, A.A. Tracer kinetic modeling of the 5-HT_{1A} receptor ligand [*carbonyl*-^{11}C]WAY-100635 for PET. *Neuroimage*, **1998**, *8*, 426-440.

[52] Andrée, B.; Halldin, C.; Pike V. W.; Gunn, R.N.; Olsson, H.; Farde, L. The PET radioligand [*carbonyl*-^{11}C]desmethyl-WAY-100635 binds to 5-HT_{1A} receptors and provides a higher radioactive signal than [*carbonyl*-^{11}C]WAY-100635 in the human brain. *J. Nucl. Med*., **2002**, *43*, 292-303.

Received: October 30, 2009 Revised: February 16, 2010 Accepted: February 16, 2010